

Vertical Resolution Enhancement of Petrophysical Nuclear Magnetic Resonance (NMR) Log Using Ordinary Kriging

Research Article

Parisa Bagheripour¹, Mojtaba Asoodeh^{1*}, Ayoob Nazarpour²

¹ Islamic Azad University, Birjand Branch, Birjand, Iran

² Drilling Department, Technical affairs, Iranian Offshore Oil Company, Tehran, Iran

Received 8 June 2013; accepted 1 August 2013

Abstract: Nuclear Magnetic Resonance (NMR) logging provides priceless information about hydrocarbon bearing intervals such as free fluid porosity and permeability. This study focuses on using geostatistics from NMR logging instruments at high depths of investigation to enhance vertical resolution for better understanding of reservoirs. In this study, a NMR log was used such that half of its midpoint data was used for geostatistical model construction using an ordinary kriging technique and the rest of the data points were used for assessing the performance of the constructed model. This strategy enhances the resolution of NMR logging by twofold. Results indicated that the correlation coefficient between measured and predicted permeability and free fluid porosity is equal to 0.976 and 0.970, respectively. This means that geostatistical modeling is capable of enhancing the vertical resolution of NMR logging. This study was successfully applied to carbonate reservoir rocks of the South Pars Gas Field.

Keywords: Nuclear Magnetic Resonance • Geostatistics • Ordinary Kriging • Resolution Enhancement • Petrophysics

© Versita sp. z o.o.

1. Introduction

Nuclear magnetic resonance (NMR) logs contain invaluable information about reservoir formations. NMR logs records can easily be converted to free fluid porosity and permeability [1, 2]. Free fluid porosity includes the pores containing fluids that are expected to flow. Permeability is defined as the capacity of a rock or sediment for fluid transmission, and is a measure of the relative ease of fluid flow under pressure gradients. Through further process-

ing, NMR log records can be converted for fluid type characterization [3] and capillary pressure curve generation [4]. There are two types of instruments used for NMR logging: one focusing on vertical resolution (six inches vertical resolution and 0.5 – 1.5 inches depth of investigation) and the other focusing on depth of investigation (5 feet vertical resolution and 14 – 16 inches depth of investigation). Actually, there is no instrument that provides both high vertical resolution and high depth of investigation. High depth of investigation captures more flow path features and gives a more representative picture of the reservoir. Meanwhile high vertical resolution provides better understanding of the rock property variations of the reservoir. Therefore, in order to reap the beneficial advantages of

*E-mail: asoodeh.mojtaba@gmail.com

both types of NMR logging tools, a strategy is needed to enhance vertical resolution of instruments with high depth of investigation.

The need for high resolution data is inevitable. However, after enhancement of vertical resolution, accuracy of generated data is important, i.e., more accurate estimation, better decision for development and production from the reservoir. Geostatistical methods are reliable and offer good accuracy for petrophysical properties estimation [5]. Geostatistics is concerned with any phenomena that change in space. It is a science that presents a combination of tools for the understanding and modeling of spatial variability [6, 7]. In this study, the Ordinary Kriging technique was used to enhance the vertical resolution of NMR logging tools with high depth of investigation. In the first stage, midpoint data from a NMR log were removed and geostatistical modeling was carried out on rest of data points. After model construction, midpoint data were estimated through the use of the developed model. This strategy was successfully applied to South Pars Gas Field of Iran. This methodology enhances the resolution of NMR log by a factor of two.

2. NMR Logging

As far back as 1946, nuclear magnetic resonance (NMR) signals from hydrogen atom nuclei (protons) were first observed independently by Purcell and Bloch, and have since been used extensively to characterize materials. Magnetic resonance imaging instruments are commonly used as diagnostic tools in medicine today. The first NMR log was run in 1960, developed by Brown and Gamson of Chevron Research Company. The tool used the Earth's magnetic field for proton alignment; the principle underlying NMR logging tools for the next 30 years [8]. NMR logging tools induces a magnetic field in reservoir layers. This field causes hydrogen protons, abundant in both water and hydrocarbons, to align in the direction of the induced magnetic field. These magnetized protons produce a signal due to the relaxation from the field direction. The NMR log measures this signal versus time and gives the T_2 relaxation or transverse relaxation distribution curve which is the basic output of NMR log which can be easily converted to free fluid porosity and permeability. Because only fluids are visible to NMR logging, the porosity measured by the tool contains no contribution from the matrix materials and does not need to be calibrated to formation lithology. This response characteristic makes NMR fundamentally different from conventional logging tools, which are mostly dominated by matrix framework and thus have higher uncertainty.

3. Area of Study: South Pars Gas Field

The data sets used in this study belong to south Pars field. The South Pars field is located in the Persian Gulf and was discovered in 1990 by drilling an appraisal well that encountered a gas reservoir in Upper Permian and Lower Triassic carbonates. This field is actually the northern extension of Qatar's North Field (Figure 1), which was discovered in 1971. The South Pars field, with 441.5 tcf proved reserve, together with its Qatari extension, North Field, with 900.5 tcf gas in place, forms the world's largest non-associated gas field. In the South Pars field, gas accumulation is mostly limited to the Permian–Triassic stratigraphic units that became prospective during the 1970s following delineation of enormous gas reserves. These units, known as the “Kangan–Dalan Formations,” constitute very extensive natural gas reservoirs in the Persian Gulf area, and are composed of a carbonate–evaporate series formerly known as the Khuff Formation. Figure 2 shows the Kangan and Dalan Formations in a stratigraphic column of South Pars Gas Field.

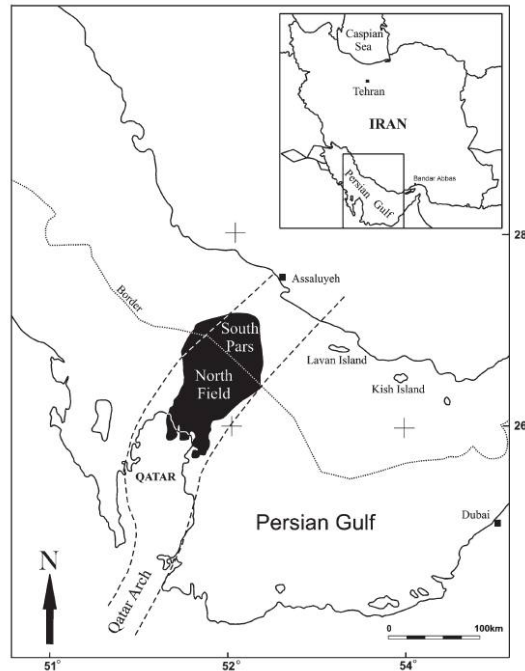


Figure 1. Location map of the South Pars field and its Qatari counterpart, the North Field, in the Persian Gulf.

| AGE | | | FORMATION | | LITHOLOGY | PET. PLAY | | | |
|-----------|-------------|----------|-----------|-------------|---|------------|------------|---|---------------------|
| MESOZOIC | L. TRIASSIC | Scythian | Dashtak | L. Sudair | Shale and Clay with Dolomitic Intercalations | Seal | | | |
| | | | | Aghar Mbr. | Shale | | | | |
| | | | Kangan | Kangan Mbr. | Shale | ☀ Gas ☀ | | | |
| | | | | K1 | Dolomite + Anhydrite Anhydrite + Dolomite | | | | |
| | | | | K2 | Dolomite Limestone | | | | |
| PALEOZOIC | PERMIAN | Upper | U-Dalan | K3 | Anhydrite + Dolomite Anhydrite | ☀ Gas | | | |
| | | | | K4 | Dolomite limestone Anhydrite + Dolomite | | | | |
| | | Middle | Nar Mbr. | | Anhydrite | | | | |
| | | | L-Dalan | K5 | Limestone + Dolomite | | | | |
| | | | | | | | | | |
| | | Lower | Faraghan | | Sandstone, Shale and Partly Limestone Basal Conglomerate | | ? ☀ Gas | | |
| | | DEVONIAN | Upper | | Zakeen | | Sandstone | ? | |
| | | | Middle | | | | | | |
| | | | Lower | | | | | | |
| | | | SILURIAN | | Lower | | Sarchahan | | Organic Rich Shales |
| | Disconf. | | | | | | | | |
| | | | | | Disconf. | | | | |

Figure 2. Stratigraphic column of the South Pars Gas Field in which the Kangan and Dalan Formations are shown in gray.

4. Geostatistics Concepts

4.1. Kriging

The field of geostatistics arises from the work of Krige [9] in the mining industry in the early 1950s and was expanded upon by Matheron [10, 11]. Geostatistics is supported by the axiom that geological data are spatially correlated [12]. By recognizing the spatial pattern of variations and applying it to unsampled locations, it is possible to estimate a sought parameter, i.e., the extracted pattern of variations determines weights of contribution of nearby samples in estimation of the value of the desired property at an unsampled location [13].

Kriging is a computational method for estimating a variable over a line (1D), area (2D) or in a volume (3D). It is a method that is based on two criteria of minimization

of variance and unbiased condition [14]. Kriging is the best linear unbiased estimator, with the exception of the Simple Kriging technique [15]. This estimator, defined as:

$$Z_k^* = \sum_{i=1}^n \lambda_i Z(x_i) \quad (1)$$

Where $Z(x_i)$ and λ_i represent the value of the sample and the weighting factor at point i , respectively. Z_k^* is the kriged estimator. The weights λ_i are calculated according to the criteria mentioned above. The ordinary kriging equation for estimation is defined as:

$$\begin{bmatrix} \gamma(\vec{x}_1, \vec{x}_1) & \cdots & \gamma(\vec{x}_1, \vec{x}_n) & 1 \\ \vdots & \ddots & \vdots & \vdots \\ \gamma(\vec{x}_n, \vec{x}_1) & \cdots & \gamma(\vec{x}_n, \vec{x}_n) & 1 \\ 1 & \cdots & 1 & 0 \end{bmatrix} \begin{bmatrix} \lambda_1 \\ \lambda_2 \\ \vdots \\ \lambda_n \\ \mu \end{bmatrix} = \begin{bmatrix} \gamma(\vec{x}_0 - \vec{x}_1) \\ \gamma(\vec{x}_0 - \vec{x}_2) \\ \vdots \\ \gamma(\vec{x}_0 - \vec{x}_n) \\ 1 \end{bmatrix} \quad (2)$$

As seen in the above equation, crucial elements of the formula are variograms that are used for calculating the differences in the desired properties between two points and generally the spatial variation of the property.

4.1.1. Variograms

Geostatistical modeling comprises two main stages: first computing and modeling the semi-variogram (extracting spatial patterns of features) and then estimating the desired variable. Continuity concept, homogeneity or heterogeneity and spatial structure of regionalized variable are recognized by (semi) variogram [16]. The semi-variogram is simply defined as half of the variance of the increments. In probabilistic form, the semi-variogram defined as:

$$\gamma(h) = \frac{1}{2} E[(Z(x+h) - Z(x))^2] \quad (3)$$

The variogram (for lag distance h) is defined as the average squared difference of pairs, separated approximately by h [10]. The following equation states this concept mathematically.

$$2\gamma(h) = \frac{1}{N(h)} \sum_{i=1}^{N(h)} [Z(x) - Z(x+h)]^2 \quad (4)$$

Where, $N(h)$ is the number of pairs for lag h .

In this study, NMR log parameters, free fluid porosity and rock permeability, constitute the sample pairs.

Variogram fitting is an iterative trial and error task that greatly depends on the experience of the geoscientist conducting the work. Therefore, some rules of thumb are suggested by several researchers for easier fitting of the variogram; however, all emphasize the fact that lesser numbers of pairs increase the uncertainty of prediction and vice versa. After choosing the appropriate minimal number of pairs, the final step in variography is modeling the variogram. The goal of the modeling is to determine the sill, slope, range, and nugget effect by use of specific theoretical functions [16]. In this stage, a proper model that best fits the experimental variogram should be chosen from among common models such as: spherical, exponential, Gaussian, linear (pure nugget effect), cubic, power, De Wijs and Cauchy [17, 18].

5. Results and Discussion

In this study, 426 midpoints of NMR records were chosen for geostatistical modeling and the points between each two successive points were estimated from the recognized pattern along the well axis (one dimensional modeling along the Z-axis). Free fluid porosity and rock permeability, that their variations' patterns are desired, do not follow a normal distribution (Figure 3). Since almost all geostatistical techniques ask for data sets with normal distributions, it is essential to transform data to a normal (Gaussian) distribution. Some attributes of normal distributions include zero mean, standard deviation of one, zero skewness and kurtosis of three. The normal score transform can transform any data distribution into the Gaussian form with a mean of zero and standard deviation of one. Table 1 shows the statistical description of free fluid porosity and rock permeability data. Figure 4 illustrates distributions of transformed data that follow exact Gaussian functions. This figure indicates the normal score transform has been successful in transforming data sets to an exact Gaussian distribution.

Experimental variograms of free fluid volume and rock permeability were calculated using WinGslib software. To initially obtain the interpretable structure, different lag distances and lag tolerances were used for calculating the variogram. Lag distances of 0.22 and 0.2 meter and lag tolerances of 0.1 and 0.11 meter were finally chosen for computing experimental variograms of free fluid porosity and rock permeability, respectively. It is worth mentioning that experimental semi-variograms were calculated by a normal score transform data set of free fluid porosity and rock permeability. After calculating the experimental variogram, theoretical models were fitted to each of them (see Figures 5 and 6). Figures 5 and 6 show that

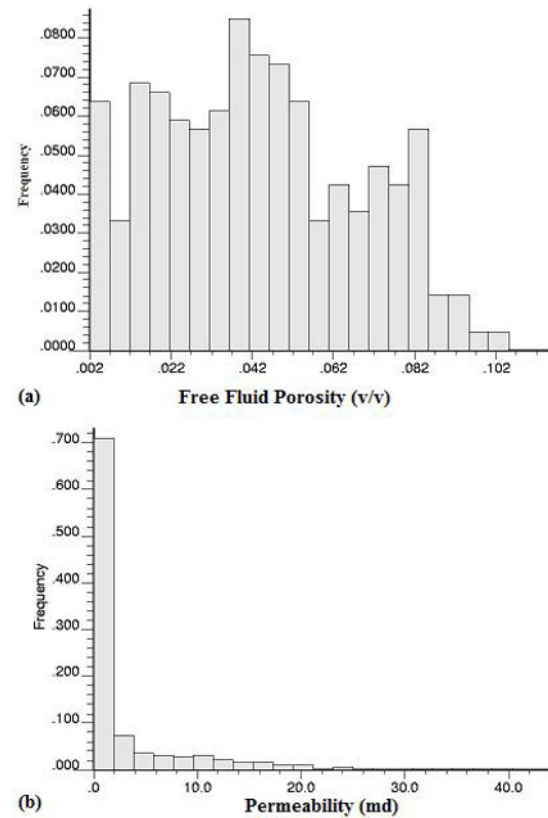


Figure 3. Histograms showing the data distribution of: (a) free fluid porosity and (b) permeability. Neither of these distributions follows a normal Gaussian function.

spherical and exponential models provide the best fit of variograms for free fluid porosity and permeability, respectively. Spherical and exponential models equations are described below:

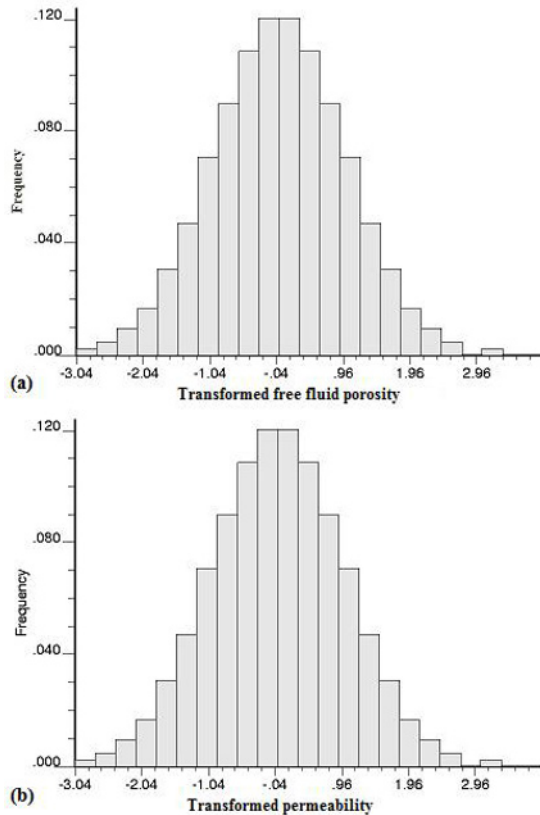
$$\gamma(h) = \begin{cases} 0.52\left(\frac{3h}{9} - \frac{h^3}{181.2}\right), & \text{if } h \leq 4.5 \\ 0.52, & \text{if } h \geq 4.5 \end{cases} \quad (5)$$

$$\gamma(h) = 0.52 \left[1 - \exp\left(-\frac{3h}{2.75}\right) \right] \quad (6)$$

An ordinary kriging algorithm with linear drift in Z direction (i.e., along well axis) was used to develop the model for estimating free fluid porosity and rock permeability in unsampled points. Figure 7 shows cross-correlation between real and geostatistically-predicted data for free fluid porosity and permeability in training data (modeling data). This figure confirms that ordinary kriging was successful in finding the z-axial pattern of NMR data. In order to test the reliability of developed models, the Jack-knife method was used. In this method, testing data are

Table 1. Descriptive statistics of free fluid porosity and permeability before and after normalization by normal score transform (Note: milli-Darcy (md) = $9.86923 \times 10^{-4} \mu\text{m}^2$).

| a) Free Fluid Porosity (fraction) | | | | | | | |
|-----------------------------------|--------|--------|---------|----------------|--------|----------------|---------|
| | Mean | STD | Max | Upper Quartile | Median | Lower Quartile | Min |
| NMR Data | 0.0433 | 0.0245 | 0.0998 | 0.0617 | 0.0413 | 0.0237 | 0.0017 |
| Normalized Data | 0.0 | 0.9985 | 3.0409 | 0.6745 | 0.0 | -0.6745 | -3.0409 |
| b) Permeability (md) | | | | | | | |
| | Mean | STD | Max | Upper Quartile | Median | Lower Quartile | Min |
| NMR Data | 3.1853 | 6.0346 | 38.4687 | 2.7128 | 0.5033 | 0.1 | 0.0033 |
| Normalized Data | 0.0 | 0.9985 | 3.0409 | 0.6745 | 0.0 | -0.6745 | -3.0409 |

**Figure 4.** Histograms showing normal distributions of transformed data: (a) Normalized free fluid porosity and (b) Normalized permeability. Normal score transforming converted both data sets to exact normal Gaussian distributions.

not used in developing the model, unlike the conventional technique known as the 'Leave-one-out' or 'cross validation' method. Figure 8 shows the cross validation between measured and predicted values of NMR log parameters, including free fluid porosity and rock permeability in test (validation) data. A comparison between measured and predicted values of NMR log parameters is presented in

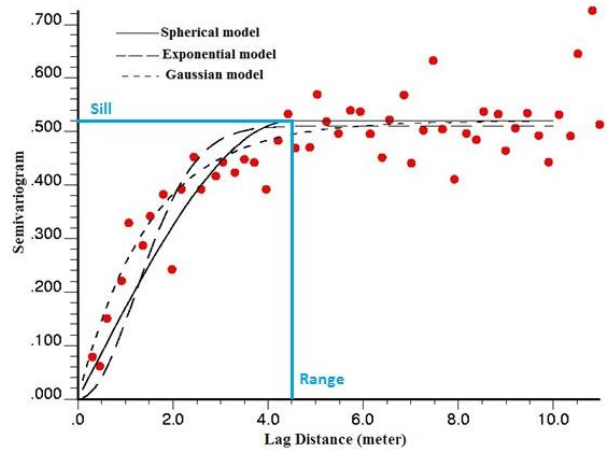
**Figure 5.** Graph showing the best theoretical model fits to the experimental variogram of free fluid porosity. The spherical model provides a better match to the variogram in this case.

Figure 9. This figure shows that geostatistics modeling enhanced the vertical resolution of the NMR log by a factor of two. This figure also shows that the accuracy of prediction is reduced in low values of free fluid porosity and permeability, which is attributed to the inherent flaw of the NMR mechanism in recording low permeability or low free fluid porosity intervals.

6. Conclusions

Processing of NMR logs provides two invaluable reservoir parameters: permeability and free fluid porosity. NMR instruments cannot provide both high vertical resolution and deep depth of investigation. This study was performed to enhance vertical resolution of NMR tools with deep depth

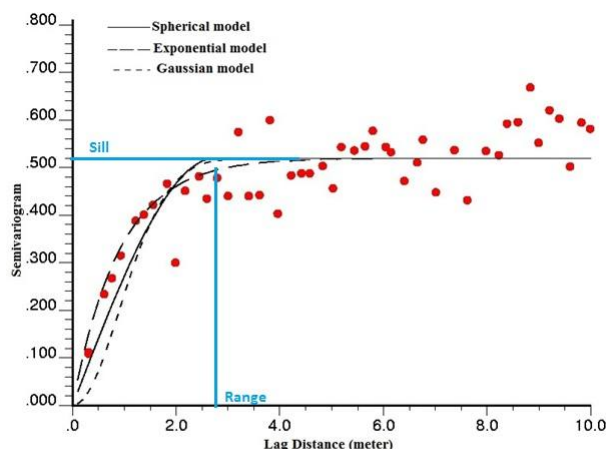


Figure 6. Graph showing the best theoretical model fits to the experimental variogram of permeability. The exponential model provides a better match to the variogram in this case.

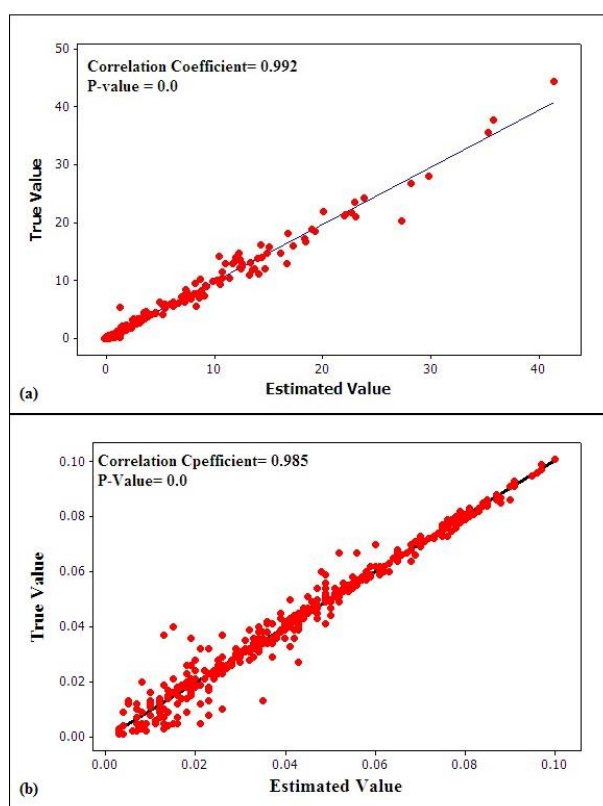


Figure 7. Graph showing correlation between measured and predicted NMR log parameters in training data: (a) free fluid porosity and (b) permeability.

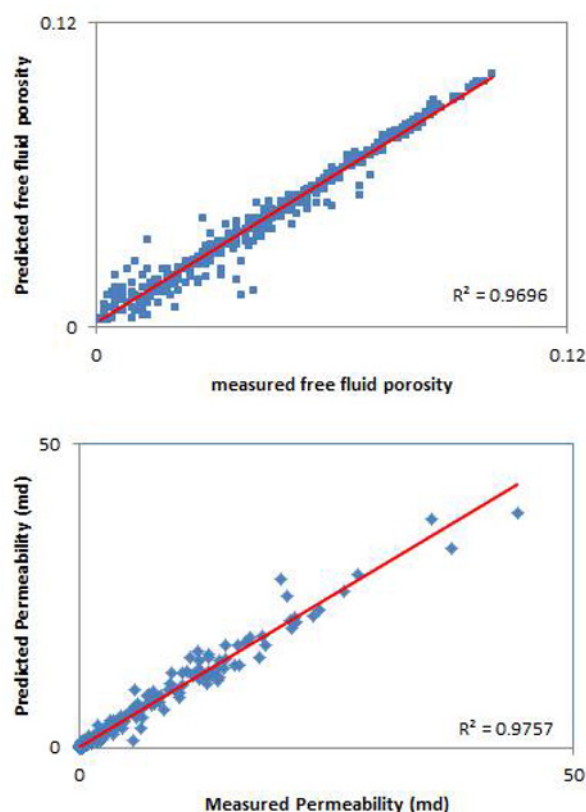


Figure 8. Graph showing correlation between measured and predicted NMR log parameters in validation data: (a) free fluid porosity and (b) permeability.

of investigation by means of the ordinary kriging method. This study shows that kriging model is capable of extracting and improving the vertical correlation of NMR log parameters, including free fluid porosity and permeability. The present study improves vertical resolution of NMR logging and breaks its magnitude in half with correlation coefficient of 0.985 and 0.992 for free fluid porosity and permeability, respectively. Estimation performance is greater in high values of permeability and free fluid porosity, which is attributed to failure of NMR logging tools to fully identify characteristics of less permeable rocks. Therefore, less permeable intervals contain noisy records, and consequently encounter higher estimation error. One should bear in mind that less permeable parts of a reservoir are due to lack of secondary processes (diagenesis) such as solution, fracturing, and dolomitization and therefore, the majority of permeability in carbonate rock is due to these secondary processes.

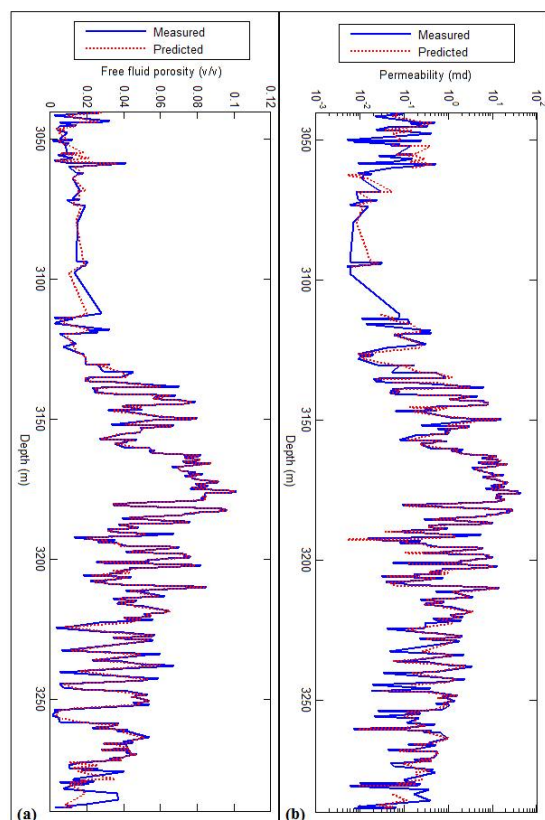


Figure 9. A comparison between measured and predicted NMR log parameters: (a) free fluid porosity and (b) permeability.

References

- [1] Xie R.H., Xiao L.Z., Dunn K J., NMR Logging Porosity Activation and Data Processing Method. *Chinese Journal of Geophysics*, 2006, 49, 1419-1424
- [2] Freedman R., Advances in NMR Logging. *JPT*, 2006, 58, 60-66
- [3] Freedman R., Heaton N., Fluid Characterization using Nuclear Magnetic Resonance Logging. *Petrophysics*, 2004, 45, 241-250
- [4] Chen S., Ostroff G., Georgi D. T., Improving Estimation of NMR Log T2 Cutoff Values with Core NMR and Capillary Pressure Measurements. In: Society of Core Analysts, Annual Conference and Exhibition, The Hague, Nederland, 1998, SCA Paper 9822
- [5] Deutsch C.V., What in the Reservoir is Geostatistics Good for?. *J. Can. Petrol. Tech.*, 45, 4, 8-13
- [6] Deutsch C.V., Journel A.G., Geostatistical Software Library and User's Guide. Second Edition, In: Oxford University Press, 1998, 53-65
- [7] Hohn M.E., Third Annual Conference of the International Association for Mathematical Geology. *Mathematical Geology*, 1999, 31, 505
- [8] Kenyon B., Kleinberg R., Straley C., Gubelin G., Morris C., Nuclear Magnetic Resonance Imaging – Technology for the 21st Century. *Oilfield Review* 3, 1995, 19-33
- [9] Krige D. G., A statistical approach to some basic mine valuation problems on the Witwatersrand. *J. of the Chem., Metal. Mining Soc. of South Africa*, 1951, 52, 119-139
- [10] Matheron G., Principles of Geostatistics. *Economic Geology*, 1963, 58, 1246-1266
- [11] Matheron G., The selectivity of the distributions and “the second principle of geostatistics”. In Verly G., et al., eds. *Geostatistics for natural resources characterization. Part 1*, Reidel, Dordrecht, 1984, 421-433
- [12] Damsleth E., Omre H., Geostatistical Approaches in Reservoir Evaluation. *JPT*, 1997, 49, 498-501
- [13] Raya P. Y., Li X.P., The Factorial Kriging Technique: a Geostatistical Tool for Acquisition Footprints Removal – A Case Study. In: Society of Exploration Geophysicists (SEG), Annual Meeting, November 9 - 14, Las Vegas, Nevada, 2008
- [14] Delfiner P., Delhomme J. P., Pelissier-Combes J., Application of geostatistical analysis to the evaluation of petroleum reservoirs with well logs. In: 24th annual logging symposium of SPWLA, June, 27-30, Calgary, 1983
- [15] Kelkar M., Perez G., Applied Geostatistics for Reservoir Characterization. Society of Petroleum Engineers Inc., 2002, 198
- [16] Hasani-pak A. A., Geostatistics. In: Tehran University Press, Tehran, 1998, 87
- [17] Yarus J. M., Chambers R. L., Practical Geostatistics – An Armchair Overview for Petroleum Reservoir Engineers. *JPT*, 2006, 58, 78-86
- [18] Dubrule O., Geostatistics for seismic data integration in earth sciences. Distinguished instructor short course, Tulsa, Okla., 2003, 26-59